Predictability of North Atlantic Tropical Cyclone Activity on Intraseasonal Time Scales

James I. Belanger*, Judith A. Curry, and Peter J. Webster

School of Earth and Atmospheric Sciences, Georgia Institute of Technology, Atlanta, GA

June 2010

Submitted to Monthly Weather Review

*Corresponding Author Address:
James I. Belanger
School of Earth & Atmospheric Sciences
Georgia Institute of Technology
311 Ferst Drive
Atlanta, GA 30332-0340
Email: james.belanger@eas.gatech.edu

Abstract

Recent work suggests that there may exist skill in forecasting tropical cyclones (TCs) using dynamically-based ensemble products, such as those obtained from the ECMWF Monthly Forecast System (ECMFS). The ECMFS features an ensemble of 51 coupled ocean–atmosphere simulations integrated to 32 days once per week. Predicted levels of TC activity in the North Atlantic Ocean with these monthly ensemble forecasts is compared to the observed variability during the months of June to October during 2008 and 2009. Results indicate that the forecast system can capture large-scale regions that have a higher or lower risk of TC activity, and has skill above climatology for the Gulf of Mexico and the Main Development Region on intraseasonal time scales. Regional forecast skill is traced to the model's ability to capture the large-scale evolution of deep-layer vertical shear, the frequency of easterly waves, and the variance in 850 hPa relative vorticity. The predictability of TC activity, along with the forecast utility of the ECMFS, is shown to be sensitive to the phase and intensity of the Madden-Julian Oscillation at the time of model initialization.

1. Introduction

Developing skillful tropical cyclone (TC) forecasts using statistical (e.g. Leroy and Wheeler 2008) and dynamical models (Bessafi and Wheeler 2006; Vitart 2009) on intraseasonal time scales has become an active research topic in recent years. Statistical methods have attempted to extract forecast predictability from the Madden-Julian Oscillation (MJO)—a convectively coupled mode of tropical atmospheric and oceanic variability that projects most strongly on the 30–60 day time scale (Madden and Julian 1972, 1994; Wheeler and Kiladis 1999). Maloney and Hartmann (2000a,b) showed that when the MJO is in its westerly, convectively active phase over the eastern North Pacific and western North Atlantic, TC activity across the Gulf of Mexico and western Caribbean Sea is enhanced. Suppressed TC activity is found to occur with the reverse orientation of the MJO: when it is in its easterly phase and its associated convective suppression is in the eastern Pacific. Maloney and Hartmann attributed this variability in TC activity to a modulation of deep-layer (850–200 hPa) westerly wind shear, whereas Camargo et al. (2009) showed that atmospheric column moistening due to the coupling of increased large-scale ascent and enhanced low-level absolute vorticity can explain the observed change in TC frequency.

Variability in the West African monsoon and the Atlantic Intertropical Convergence Zone (ITCZ) have also been shown to impact the intraseasonal variability of TCs in the tropical Atlantic (Maloney and Shaman 2008). Generally, TC activity in the eastern North Atlantic is suppressed (enhanced) 5–10 days before (after) a maximum in intraseasonal precipitation across the West African monsoon region. Maloney and Shaman attribute the modulation of TC activity to variations in vertical wind shear, where a difference of more than 6 m s^{-1} was found between active and suppressed precipitation periods. Since the MJO regulates roughly 30% of the total variance in the intraseasonal precipitation anomalies across the region, Maloney and Shaman find that the MJO modulates the regional vertical wind shear variations to a large degree as well.

Although Maloney and Shaman's results support the TC–vertical wind shear relationship found on longer time scales (i.e., interannual to multidecadal; Landsea and Gray 1992; Goldenberg et al. 2001; Bell and Chelliah 2006), additional factors are likely relevant to TC variability on intraseasonal time scales, such as variations in African easterly waves (AEWs). While easterly wave activity on interannual time scales is weakly related to TC frequency in the MDR (Frank 1975; Thorncroft and Hodges 2001; Hopsch et al. 2007), it is hypothesized that variations in AEW activity modulate enhanced or suppressed periods of tropical cyclone activity in the North Atlantic on intraseasonal time scales. This hypothesis is in keeping with Maloney and Shaman (2008) who provide evidence that AEW activity may be an important factor on intraseasonal time scales, as their regression analyses of eddy vorticity and winds during intraseasonal periods of strongest eddy kinetic energy produced structures resembling AEWs with zonal wavelengths of 2500 km and a southwest–northeast tilt with latitude.

To explore how phasing of the MJO impacts tropical cyclone frequency in the ECMWF Monthly Forecast System (ECMFS), Vitart (2009) conducted hindcast experiments from 1989 to 2008 using an ensemble of 15 members that were initialized on the 15th of each month and run for 46 days. Using the Wheeler-Hendon (2004) MJO Index, the model simulations showed an increase (decrease) of TC activity across the Atlantic during MJO Phases 2–3 (6–7), which is in qualitative agreement with observations but with a weaker MJO impact than is seen in observations. Vitart (2009) also showed that MJO phasing projects onto the risk of landfall, as determined by the accumulated cyclone energy over land, with MJO Phases 2–3 leading to higher risk of landfall than MJO Phases 6–7. Although Vitart's study highlights the ability of the dynamical-modeling system to produce intraseasonal TC variability based on MJO phasing in

agreement with observations, additional work is required to understand the predictability of TCs on intraseasonal time scales and the current limitations of these extended forecasts.

In this study, we evaluate the forecast skill of TC predictions for the tropical North Atlantic using the ECMFS. Since the ECMFS can reproduce the observed variability of the MJO realistically through three weeks (Vitart 2009), it is expected that this system is capable of reliably identifying periods in a forecast cycle that should portend higher or lower TC activity than normal. After introducing the data and methodology, results from the ECMFS during the 2008 and 2009 Atlantic hurricane seasons are presented along with findings of a predictability analysis of the large-scale environment. Finally, a summary of the potential implications from this research is given in Section 4.

2. Data and Methodology

This study examines North Atlantic tropical cyclones and the large-scale environment within which they are embedded for the period June–October of 2008–2009. The analysis employs forecasts from the ECMFS, the ERA-Interim reanalysis, and observations of tropical cyclone tracks from the HURricane DATabase (HURDAT).

HURDAT consists of 6-hour location coordinates and maximum intensity estimates of tropical or subtropical systems that obtained tropical storm strength or greater and is updated annually by the National Hurricane Center (Neumann et al. 1999). For this analysis, we isolate the 6-hour location coordinates for each tropical cyclone when the system was of tropical depression strength or greater. The ECMFS is an extension of the Variable Ensemble Prediction System (Buizza et al. 2007), which consists of 50 perturbed members plus a control simulation of the ECMWF general circulation model at TL399 (horizontal resolution about 50 km) with 62 vertical levels for the first ten days. For days 11–32, the model integrations occur at a reduced TL255 spectral truncation or a horizontal resolution of 80 km. At day 10, the atmospheric model is coupled to the Hamburg Ocean Primitive Equation (HOPE) model, which has 29 vertical levels, a zonal resolution of 1.4^{o}, and a meridional resolution that varies from 0.3^{o} near the equator to 1.4^{o} poleward of 30^{o}. To represent the uncertainty in initial conditions, ensemble perturbations are constructed using singular vectors, which capture the fastest growing errors in the first 48 hours (Buizza and Palmer 1995), and stochastic perturbations are added during the model integration to account for the uncertainty in parameterized physical processes. Five additional singular vectors are computed and perturbed in the six grid spaces enclosing each TC using a diabatic, adjoint version of the ECMWF global atmospheric model at TL42 spectral truncation with 42 vertical levels (Barkmeijer et al. 2001, Puri et al. 2001).

To identify tropical cyclones in the model analysis and forecast fields, a TC tracking scheme based on Vitart et al. (1997) is used. The scheme locates maxima of 850 hPa relative vorticity greater than 3.5×10^{-5} s^{-1} along with local minima in sea-level pressure. The thermal structure from 500 to 200 hPa is then determined to confirm that a warm core center is in proximity with the identified TC center ($\leq 2^{o}$) and that the temperature from the warm core center decreases outward by at least 0.5^{o}C within 8^{o} latitude distance. The purpose of imposing this warm core requirement is to ensure that extratropical cyclones are not included in the TC tracking results. TC intensity at 6-hour intervals is determined using the maximum 850 hPa wind speed.

After applying the tropical cyclone tracking scheme to the output from the ensemble forecast system, gridded probabilistic forecasts are constructed by translating the ensemble tropical cyclone tracks for a particular time period onto a $0.25^{o} \times 0.25^{o}$ grid. The local probability is determined by first summing the number of unique ensemble member tracks that are located within 2.5^{o} of each grid point, and then normalizing by the total number of forecast runs (i.e. 51). To evaluate the skill of the probabilistic forecasts, gridded track observations are constructed in a similar manner to the probability forecasts. Observed TC tracks for a specified time period (e.g. the full 32 days) are transferred to the same regular grid as the probability forecasts. A value of one or zero is given to each grid point if a TC was found or not found within 2.5^{o} of that site. The 2.5^{o} threshold was selected to ensure some measure of spatial homogeneity in the forecast skill assessment since the number of unique monthly forecasts is limited to only the 2008 and 2009 summer seasons.

In addition to tracking TCs in the ECMFS, we analyze the trajectory and intensity of African easterly waves using a Hovmöller method developed by Agudelo et al. (2010). The easterly wave tracking algorithm uses 2 – 6 day Fourier filtered, westward-moving 850 hPa relative

vorticity for the latitudinal averaged band of 5°-15°N. Based on the timing and location of the local maximum of 850 hPa relative vorticity that pass across 20°W, a recursive algorithm is applied to identify the longitudinal extent of the easterly wave as a function of time. For this analysis, the impact of the forecast frequency of AEWs on the predicted levels of tropical cyclone activity in the ECMFS will be evaluated.

To assess the predictability of TC activity in the ECMFS on intraseasonal time scales, we use the Brier skill score (BSS), relative operating characteristic (ROC), and the reliability diagram. The BSS measures the accuracy or relative skill of a forecast over climatology by predicting whether or not an event will occur in comparison to observations and is defined as:

$$BS = \frac{1}{N}\sum_{i=1}^{N}\left(p_i - \delta_i\right)^2 \quad (1)$$

$$BSS = 1 - \frac{BS}{BS_{ref}}, \quad (2)$$

where N is the number of forecasts, i is the i^{th} forecast, p is the forecast probability, δ is a value of 1 or 0 depending on whether the event occurred, and BS_{ref} is the Brier score of climatology (Brier 1950; Wilks 1995).

Since other performance measures may reveal higher forecast skill than the BSS (Mason 2004), we also use ROC scores and reliability diagrams in the verification analysis. The ROC is a comparison of the hit rate and false alarm rate for a set of increasing probability thresholds and is therefore an assessment of the forecast skill conditioned on the observations. The hit rate, or the probability of detection, is the proportion of all forecasts where a forecast warning was issued correctly, and the false alarm rate, or the probability of false detection, is the proportion of all forecasts where a forecast warning was issued and did not occur along with the number of correction rejections (Wilks 1995; Mason and Graham 1999). The area under the ROC curve, known as the ROC score, is a value from 0 to 1, where 0.5 indicates no forecast skill and a value of 1 is a perfect forecast system (Mason and Graham 1999). Besides assessing the forecast performance conditioned on the observations, we also evaluate the reliability of the forecasts by determining how well observations correspond with each forecast probability category. The conditional bias is shown graphically through the reliability (or attributes) diagram where high reliability is indicated by close proximity to the diagonal (Wilks 1995).

3. Results and Discussion

Tropical cyclone activity predicted from the ECMFS is compared with TC climatology (1970 – 2000) for the forecasts initialized on 7 August 2008 and 14 August 2008 (Figs. 1a-b). For the 7 August 2008 forecast, lower than normal TC activity was projected to occur across much of the North Atlantic. However, the monthly forecast issued just one week later indicated that the subsequent 32-day forecast period would be quite active, especially across much of the northern Main Development Region (MDR; 20°– 60°W, 10°–20°N) and the Greater Antilles. Observations from HURDAT for this time period indicated that five TCs developed (i.e. Tropical Storm Fay, Hurricane Gustav, Hurricane Hanna, Hurricane Ike, and Tropical Storm Josephine) and moved through the tropical North Atlantic region that was forecast on 14 August 2008 to see higher than normal TC activity but one week prior was forecast to be below normal.

To explain the weekly variability in predicted levels of TC activity in the ECMFS, we hypothesize that both the phasing (Vitart 2009) and the amplitude of the MJO modulates the projected levels of TC activity in the model and ultimately regulates which intraseasonal predictions will be more skillful than others. In the case of Fig. 1a (7 August 2008), the MJO projection onto the Wheeler-Hendon phase space was weak and centered in the Indian Ocean. However, the convectively active phase on 14 August 2008 was strong and remained centered in the Indian Ocean, which provides anecdotal evidence of this forecast sensitivity. This hypothesis is evaluated more formally in Section 3c.

a) Skill of the Monthly Forecast System

To provide an evaluation of the ECMFS skill, spatial Brier skill scores are shown in Figs. 2a-d for all of the monthly forecasts produced weekly from June to October during 2008 and 2009. For each composite, the reference forecast is the climatology of tropical cyclone activity from 1970–2000 using HURDAT and varies based on the specific time period covered by each monthly forecast. To show the temporal sensitivity of the forecast skill, the analysis for the monthly forecast period is divided by the number of weeks-in-advance (e.g., Week 1 includes forecast days 1-7; Week 2: days 8-14; Week 3: days 15-21; Week 4: days 22-28). [Note that the ECMWF defines their weekly periods differently so that the full 32-day forecast is covered by a four-week period with the same model resolution (Vitart et al. 2008).] From Figures 2a and 2b, it is seen that the ECMFS produces skillful predictions of tropical cyclone activity across much of the tropical North Atlantic including the MDR (20°– 60°W, 10°–20°N), West Atlantic (60°–90°W, 20°–35°N), northern Caribbean Sea, and the Gulf of Mexico. For Week 3, the regions of positive Brier Skill Scores narrows and is focused in the southern Gulf of Mexico and central MDR. By Week 4, the central MDR is the only region of the tropical North Atlantic that features skill above climatology. Finding skill especially for Weeks 3 and 4 in the MDR is surprising since the major source of predictability beyond two weeks is the MJO, and the observed impact of MJO variability on TC activity is focused in the Gulf of Mexico and western Caribbean Sea (Maloney and Hartmann 2000a,b; Klotzbach 2010). Possible explanations for this long-lead forecast skill in the central MDR are provided in Section 3b.

Consistency of the probabilistic forecasts is investigated using the reliability diagram along with the occurrence frequency of each forecast probability level (Fig. 3). The ECMFS overforecasts (i.e., TC forecast probabilities too high) for all probability levels and across all weekly periods. Although the composite reliability of the Week 1 forecasts increases linearly as the forecast probability level increases, the composite reliability of the Week 2–4 forecasts reaches a plateau near 40–50% and only agrees with observations approximately 20% of the time. Since the occurrence frequency of forecast probability levels rarely exceeds 50% for these

longer lead-time forecasts (i.e., Weeks 2-4), it is unclear whether this reliability plateau represents a dynamical predictability limit or is due simply to an insufficient sample size of monthly forecasts. Unlike a climatology forecast that provides no resolution (Wilks 1995), the ECMFS provides moderate resolution in that it can discriminate between TC events and nonevents across all weekly periods.

The ECMFS's ROC for TC activity complements the reliability diagram. Given the spatial and temporal differences in Brier skill scores (Figs. 2a-d), the ROC is calculated regionally using the maximum TC forecast probability as a function of weeks-in-advance in four regions: the Gulf of Mexico, Caribbean Sea, West Atlantic, and Main Development Region (Figs. 4a-d). Table 1 provides the regional ROC scores for Weeks 1–4. The ROC scores are calculated by integrating the hit rates for each region as a function of increasing false alarm rates. A ROC score of 0.5 indicates no forecast skill and a value of 1.0 characterizes a perfect prediction. For the Week 1 forecasts, the Gulf of Mexico, West Atlantic, and Main Development Region have the highest ROC scores (0.85–0.87) with low false alarm rates and high probabilities of detection as a function of increasing probability level (Fig. 4). For the Week 2 forecasts, the West Atlantic and Main Development Region maintain moderate to high forecast skill with ROC scores around 0.8, while the forecasts for TC activity in the Gulf of Mexico have the largest decrease from Week 1 to Week 2 (from 0.85 to 0.66). For the Week 3 and 4 forecasts, ROC scores average around 0.65 for the Gulf of Mexico, Caribbean Sea, and West Atlantic with higher forecast skill in the Main Development Region (ROC score ~ 0.75). Since the ECMFS ROC scores remain above 0.5 through four weeks, this result indicates that forecast skill exists across all regions and for all time periods considered even though the BSS analyses in Fig. 2 imply that the MDR and Gulf of Mexico are the only regions that feature forecast skill on time scales longer than two weeks.

b) Predictability of the large-scale environment

Since large-scale environmental variables explain at least 50% of the total variance in TC genesis events across the tropical North Atlantic (Agudelo et al. 2010), the predictability of the large-scale environmental flow is evaluated to explain why forecast skill utilizing the ECMFS exists on intraseasonal time scales across the tropical Atlantic. The analysis focuses on the ability of the model to capture the variability in deep-layer vertical wind shear (850-200 mb), the frequency of AEWs, and the variance in 850 hPa relative vorticity. Other environmental variables such as column integrated humidity, upper (lower) level divergence (convergence), large-scale vertical velocity, or mid-latitude trough interactions may also be relevant, but their importance remains a topic of future work.

Spatial correlation coefficients between forecast values of deep-layer vertical wind shear and observations as determined by the ERA-Interim reanalysis (Uppala et al. 2007) are given in Figs. 5a-d as a function of weeks-in-advance. The ERA-Interim dataset (horizontal resolution of 1^{o} latitude/longitude) is an updated reanalysis of ERA-40 that covers the time period from 1988 to present. The correlation coefficients are calculated using the mean 12-hour correlation coefficients during each week of the monthly forecast period. Correlation coefficients exceed 0.8 for most regions of the tropical Atlantic including the MDR, West Atlantic, and the Gulf of Mexico for Week 1. In Weeks 2–4, the Gulf of Mexico and the MDR have the highest correlations, as the forecast system captures one-third of the total variance in vertical wind shear. On the other hand, the lowest predictability is found in the eastern Caribbean Sea. Given the close correspondence between regions of positive Brier Skill Scores, high ROC scores, and moderate to high correlation coefficients for vertical wind shear, this result suggests that forecast

skill for tropical cyclones especially in the central MDR and West Atlantic may be due to accurate vertical wind shear forecasts.

The inability of the ECMFS to reproduce the observed variance in vertical wind shear in the Caribbean Sea, as seen in Week 3 and Week 4 (Figs. 5c-d), is tied to variability in the intensity of the tropical upper-tropospheric trough, as this region exhibits more variance in vertical wind shear than any other location in the tropical North Atlantic (not shown). Vertical wind shear is thought to inhibit TC genesis and intensification by increasing ventilation (Gray 1968), by modifying vertical stability (DeMaria 1996), and by inducing changes in the secondary circulation (Bender 1997). The relationship between vertical wind shear variations in the tropical Atlantic and TC frequency on intraseasonal time scales has been discussed by Mo (2000), Maloney and Shaman (2008), and Vitart (2009).

The impact of AEW frequency on tropical North Atlantic TC predictions by the ECMFS is evaluated as a potential contributor to the intraseasonal forecast skill. The application of the modified AEW tracking scheme by Agudelo et al. (2010) to the ECMFS from 2008 and 2009 shows that the impact of AEW variability is largest for most of the MDR and throughout the Gulf of Mexico (Fig. 6a). For these regions, about 25% of the total variance in tropical cyclone activity may be attributed to the forecast frequency of AEWs. In addition, the spatial pattern of covariability coincides with the regional locations that have skillful TC forecasts (i.e., positive Brier skill scores and high ROC scores), which suggests that the forecast frequency of AEWs is an important component in the intraseasonal predictions of TCs in the ECMFS.

The ability to reproduce the variability in low-level relative vorticity is inherent to the predictability of the large-scale environmental flow, as ambient vorticity is a necessary condition for TC seedling growth and development especially from AEWs (Berry and Thorncroft 2005). The correlation coefficients between the predicted variance in 850 hPa relative vorticity in the MDR and the observed variance from the ERA-Interim reanalysis are shown in Figs. 5b-d for the years 2008–2009. During June–October 2008, the correlation coefficients drop below statistically significant values (< 95% confidence level) after day 10, but then increase from zero to about 0.45 during Weeks 3–4. Whereas the predictability of the variance in 850 hPa relative vorticity for the MDR was limited to Week 1 during 2008, variability in low-level relative vorticity for 2009 was much more predictable (out to four weeks) especially across much of the eastern MDR, which coincides with a region that had positive Brier skill scores (Fig. 2) and moderate to high ROC scores (Fig. 4d). This interannual difference may reflect the impact of the El-Niño Southern Oscillation (ENSO) on tropical Atlantic predictability, as El Niño conditions prevailed throughout much of the 2009 hurricane season, whereas ENSO neutral conditions occurred during 2008.

c) Relationship with the Madden-Julian Oscillation

Forecast sensitivity to the phasing and intensity of the MJO is examined as another source of variability in the TC forecasts from the ECMFS. Mean TC probability forecasts of the ECMFS based on the location at the time of model initialization of the MJO in the Indian Ocean (Phases 1–3), West Pacific (Phases 4–5), and the East Pacific/Atlantic (Phases 6–8) are shown in Figs. 7a-c, respectively, provided the MJO had an amplitude of at least one standard deviation. Since the impact of MJO phasing in the model forecast is sensitive to the seasonal climatology of TC activity across the North Atlantic, this impact is accounted for in Figs. 7d–f, which are the mean TC forecasts after the 32-day TC climatology for each monthly prediction has been removed. When the MJO is centered in the Indian Ocean (Fig. 7a) at the time of model initialization, the ECMFS will typically predict elevated levels of TC activity during the following 32-day period

in a region emanating from the MDR and stretching into the Caribbean Sea, West Atlantic, and Gulf of Mexico. If these cases are adjusted by the seasonal climatology of TCs (e.g., Fig. 7d), the anomalous elevation in TC activity is confined mainly to the MDR and north of the Greater Antilles. For time periods when the MJO is located in the West Pacific (Fig. 7b), elevated levels of TC activity across the tropical Atlantic are reduced and confined to the western Caribbean and the eastern MDR. When adjusted by the seasonal TC climatology, the predicted level of TC activity across much of the West Atlantic is suppressed relative to climatology (Fig. 7e). When the MJO is initially located in the East Pacific/Atlantic (Fig. 7c), elevated TC activity is confined only to the western Caribbean Sea and the southern Gulf of Mexico, which is consistent if the TC forecasts are adjusted by the seasonal climatology (Fig. 7f). These forecast tendencies are in agreement with previous observational and modeling studies on the relationship between MJO phasing and Atlantic TC activity (Mo 2000; Barrett and Leslie 2009; Vitart 2009; Klotzbach 2010).

If the sensitivity analysis to MJO phasing is completed for the ECMFS forecasts when the MJO amplitude is less than one standard deviation, no significant departure from TC climatology is found across the tropical Atlantic except for MJO Phases 4–5 in which TC activity in the MDR, Caribbean Sea, and Gulf of Mexico is well below climatology (not shown). These results indicate that in addition to MJO phasing (Vitart 2009), the initial amplitude of MJO at the time of model initialization also modulates which regions of the tropical Atlantic will have enhanced or suppressed TC activity.

From an operational perspective, knowing how the predicted levels of TC activity in the ECMFS will vary based on phasing of the MJO is insightful. However, this knowledge does not provide any guidance as to whether a forecast is reliable. Forecast utility based on MJO phasing and intensity is displayed in Fig. 8 in terms of the conditional reliability of the intraseasonal forecasts, which is based on regional clusters of the MJO location at the time of model initialization and for events when the amplitude of the MJO as determined by Wheeler-Hendon MJO index is at least one standard deviation. The most reliable forecasts (i.e.,close proximity to the diagonal line) occur when the MJO is initially in the Indian Ocean (Phases 1–3). During the June to October period for 2008–2009, 42% of all the weekly forecasts were initialized when the MJO was initially centered in this region, and for this condition, the model provides excellent reliability for forecast TC probability levels from 0% to 40%. Between the forecast thresholds of 50% to 80%, the forecasts of Atlantic TC activity have no significant improvement over the 40% threshold. However, the probability levels from 80% to 100% tend to be more reliable, as they verify 50% to 80% of the time, respectively.

Outside of the time periods when the MJO is initially located in the Indian Ocean, the reliability of the ECMFS forecasts of TC activity are significantly limited (Fig. 8). When the MJO is either located in the western North Pacific (Phases 4–5) or the Western Hemisphere (Phases 6–8), forecast probability levels of TC activity between 0% and 60% are in agreement with observations less than 20% of the time, which in fact is even less reliable than a TC climatology forecast (not shown). Although reliability beyond the 60% forecast probability level increases, this apparent improvement in forecast utility is likely an artifact of the limited sample size for cases that exceed 60% (see Fig. 8 inset). From this reliability analysis in conjunction with the spatial composites of TC activity conditioned on the phase of the MJO, Atlantic TC predictability on intraseasonal time scales using the ECMFS appears to reside during time periods when the MJO is convectively active and initially located in the Indian Ocean.

One caveat to these results is that they are based on only two years of data with one year (2009) have lower than normal MJO variability. The amplitude of the MJO during June–October 2008 was on average larger than in 2009 with the active convective phase located mostly in Phases 1–3 during 2008 (Figs. 9a-b). Although these two seasons provide some indication on how Atlantic TC activity in the ECMFS may respond to the MJO, a larger sample of monthly forecasts that includes greater MJO variability along with unique background states (i.e., ENSO) is needed to confirm this sensitivity.

4. Conclusions

The predictability of TC activity in the tropical North Atlantic using the ECMWF Monthly Forecast System has been evaluated in terms of Brier skill scores, regional relative operating characteristic scores, and reliability diagrams to determine the conditional bias of the forecast scheme. From the Brier skill score analysis, the tropical Atlantic regions that have forecast skill include the Main Development Region, West Atlantic, northern Caribbean Sea, and Gulf of Mexico during the first two weeks. For Week 3 forecasts, forecast skill is only found for the southern Gulf of Mexico and Main Development Region, and at longer lead times the only skill is in the central MDR. Regional weekly ROC scores indicate that Week 1 forecasts have low false alarm rates for most regions of the tropical Atlantic (excluding the Caribbean Sea) and increasing probabilities of detection as the decision threshold is increased. Even at longer time scales, the four regions have forecast skill through Week 3 and Week 4 with average ROC scores of 0.75 for the MDR and 0.65 for the Gulf of Mexico, Caribbean Sea, and West Atlantic.

To evaluate why the ECMFS is able to produce skillful TC forecasts on intraseasonal time scales, the model's ability to forecast vertical wind shear is examined. For the Gulf of Mexico and MDR, the monthly forecasts explain nearly one-third of the observed variability in deep-layer vertical wind shear through four weeks. The regions of positive BSS and high ROC scores as a function of time coincide with the same regions as high vertical wind shear predictability.

We also determine whether the frequency of AEWs modulates TC predictions from the ECMFS. Although on interannual time scales AEW frequency only weakly impacts North Atlantic TC frequency (Frank 1975; Thorncroft and Hodges 2001; Hopsch et al. 2007), around 25% of the total variance in TC activity predicted by the ECMFS is associated with the frequency of AEWs. Furthermore, the spatial pattern of higher covariability values coincides with regional locations that featured skillful TC forecasts, including the Gulf of Mexico and the Main Development Region, which indicates that AEW frequency is an important contributor on intraseasonal time scales. Although this analysis has shown that vertical wind shear variability and easterly wave activity impacts Atlantic TC predictability in the ECMFS, additional research is still necessary to determine the role of other environmental variables such as column integrated specific humidity, upper (lower) level divergence (convergence), and mid-latitude trough interactions.

Following Vitart (2009), phasing and amplitude of the MJO are considered to modulate TC predictions in the tropical Atlantic and, ultimately, their reliability. When the MJO is centered in the Indian Ocean at the time of model initialization, the ECMFS will typically predict elevated levels of TC activity during the 32-day forecast period in a region from the Main Development Region into the West Atlantic. When the MJO is located in the West Pacific, the ECMFS predicts TC activity will be below climatology in the western North Atlantic. When the active convective phase of the MJO is in the Western Hemisphere, elevated TC probability levels according to the ECMFS are confined to the western Caribbean and southern Gulf of Mexico. These results are qualitatively consistent with Vitart (2009) who found MJO Phases 2–3 (6–7) at the time of model initialization cause an increase (decrease) of TC activity across the North Atlantic. When the reliability analysis of the ECMFS is conditioned on MJO location and amplitude, the most reliable TC forecasts from the model occur when the convectively active MJO is initially located in the Indian Ocean. The dynamical interpretation is that because the MJO propagates slowly, when the convectively active phase is over the Indian Ocean (Phases 2 and 3), favorable environmental conditions for TC formation will generally occur in the Atlantic for at least the first two weeks of the prediction. When the MJO is not centered in the Indian

Ocean at the time of model initialization, reliability is significantly degraded as forecast probability levels between 0% and 60% verify less than 20% of the time with observations. Since the sensitivity analysis of the ECMFS to the MJO uses only two years of data with 2009 having lower MJO variability than 2008, additional research is necessary to verify these results with a larger sample of monthly forecasts forced from unique climate states and with greater MJO variability.

The findings from the spatial skill analysis in conjunction with work by Vitart (2009) provide evidence that dynamically–based TC forecasts on intraseasonal time scales can be produced for the tropical North Atlantic. Further research is still needed to identify whether it is possible to extract additional TC predictability information from the MJO by improving how the ECMFS propagates a weaker MJO signal. Even considering the current dynamical model limitations, a statistical-dynamical method might be developed in which intraseasonal forecasts of TC activity in the tropical Atlantic would utilize these dynamical predictions during times when the MJO is convectively active and initially located in the Indian Ocean. During other time periods when the ECMFS is expected to be less reliable, statistical methods (e.g., Leroy and Wheeler 2008) could be applied. Since Maloney and Shaman (2008) have linked intraseasonal precipitation variability of the West African Monsoon and Atlantic ITCZ to TC frequency in the tropical Atlantic, further research is warranted to understand whether the ECMFS is capable of predicting this additional source of intraseasonal variability and its impact on tropical Atlantic TC activity.

Acknowledgments

The authors would like to thank Hai-Ru Chang for downloading and processing the ECMWF data, Paula Agudelo for her help with the easterly wave tracking algorithm, and Mark Jelinek for his helpful suggestions during manuscript preparation. In addition, we appreciate continuing interactions with Dr. Frederic Vitart and his colleagues at ECMWF. Funding support for this research was provided by the Climate Dynamics Division of the National Science Foundation under grant NSF 0826909.

410 **References**

411 Agudelo P. A., C. D. Hoyos, J. A. Curry, and P. J. Webster, 2010: Probabilistic discrimination
412 between large-scale environments of intensifying and decaying African easterly waves, *Clim.*
413 *Dyn*.: In press
414 Barkmeijer, J., R. Buizza, T. N. Palmer, K. Puri, and J.-F. Mahfouf, 2001: Tropical
415 singular vectors computed with linearized diabatic physics. *Quart. J. Roy. Meteor.*
416 *Soc.*, **127**, 685-708.
417 Barrett, B. S., and L. M. Leslie, 2009: Links between tropical cyclone activity and Madden-
418 Julian Oscillation phase in the North Atlantic and Northeast Pacific basins. *Mon. Wea. Rev.*, **137**,
419 727–744.
420 Bell, G. D., and M. Chelliah, 2006: Leading modes associated with interannual variability and
421 multidecadal fluctuations in North Atlantic hurricane activity. *J. Climate*, **19**, 590–612.
422 Bender, M. A., 1997: The effect of relative flow on the asymmetric structure in the interior of
423 hurricanes. *J. Atmos. Sci.*, **54**, 703–724.
424 Berry, G. J., and C. Thorncroft, 2005: Case study of an intense African easterly wave. *Mon. Wea.*
425 *Rev.*, **133**, 752–766.
426 Brier, G. W., 1950: Verification of forecasts expressed in terms of probability. *Mon. Wea. Rev*.,
427 **78**, 1–3.
428 Buizza, R., J. R. Bidlot, N. Wedi, M. Fuentes, M. Hamrud, G. Holt, and F. Vitart,
429 2007: The new ECMWF VAREPS (VAriable Resolution Ensemble Prediction System).
430 *Quart. J. Roy. Meteor. Soc.*, **133**, 681-695.
431 Buizza, R., and T. N. Palmer, 1995: The singular vector structure of the atmospheric
432 global circulation. *J. Atmos. Sci.*, **52**, 1434-1456.
433 Camargo, S. J., M. C. Wheeler, and A. H. Sobel, 2009: Diagnosis of the MJO modulation of
434 tropical cyclogenesis using an empirical index. *J. Atmos. Sci.*, **66**, 3061–3074.
435 DeMaria, M., 1996: The effect of vertical shear on tropical cyclone intensity change. *J. Atmos.*
436 *Sci*., **53**, 2076–2087.
437 Frank, N., 1975: Atlantic tropical systems of 1974. *Mon. Wea. Rev.*, **103**, 294–300.
438 Goldenberg, S. B., C. W. Landsea, A. M. Mestas-Nuñez, and W. M. Gray, 2001: The recent
439 increase in Atlantic hurricane activity: Causes and implications, *Science*, **293**, 474–479.
440 Gray, W. M., 1968: Global view of the origin of tropical disturbances and storms. *Mon. Wea.*
441 *Rev.*, **96**, 669–700.
442 Hopsch, S. B., C. D. Thorncroft, K. Hodges, and A. Aiyer, 2007: West African storm tracks and
443 their relationship to Atlantic tropical cyclones. *J. Climate*, **20**, 2468–2483.
444 Klotzbach, P. J., 2010: On the Madden-Julian Oscillation-Atlantic hurricane relationship. *J.*
445 *Climate*, **23**, 282–293.
446 Landsea, C. W., and W. M. Gray, 1992: The strong association between western Sahel monsoon
447 rainfall and intense Atlantic hurricanes. *J. Climate*, **5**, 435–453.
448 Leroy A., and M. C. Wheeler, 2008: Statistical prediction of weekly tropical cyclone activity in
449 the Southern Hemisphere. *Mon. Wea. Rev.*, **136**, 3637–3654.
450 Madden, R. A., and P. R. Julian, 1971: Detection of a 40–50 day oscillation in the zonal wind in
451 the tropical Pacific. *J. Atmos. Sci.*, **28**, 702–708, doi: 10.1175/1520-
452 0469(1971)028<0702:DOADOI>2.0.CO;2.
453 Majumdar, S. J., and P. M. Finocchio, 2010: On the ability of global Ensemble Prediction
454 Systems to predict tropical cyclone track probabilities. *Wea. Forecasting*: In press

Maloney, E. D., and D. L. Hartmann, 2000a: Modulation of eastern North Pacific hurricanes by the Madden-Julian Oscillation, *J. Climate*, **13**, 1451–1460, doi:10.1175/1520-0442(2000)013<1451:MOENPH>2.0.CO;2.

Maloney, E. D., and D. L. Hartmann, 2000b: Modulation of hurricane activity in the Gulf of Mexico by the Madden-Julian Oscillation. *Science*, **287**, 2002–2004, doi:10.1126/science.287.5460.2002.

Maloney, E. D., and J. Shaman, 2008: Intraseasonal variability of the West African monsoon and Atlantic ITCZ. *J. Climate*, **21**, 2898–2918, doi:10.1175/2007JCLI1999.1.

Mason, S. J., and N. E. Graham, 1999: Conditional probabilities, relative operating characteristics, and relative operating levels, *Wea. Forecasting*, **14**, 713-725.

Mason, S. J., 2004: On using "climatology" as a reference strategy in the Brier and ranked probability skill scores. *Mon. Wea. Rev.*, **132**, 1891–1895.

Mo, K. C., 2000: The association between intraseasonal oscillations and tropical storms in the Atlantic basin. *Mon. Wea. Rev.*, **128**, 4097–4107, doi:10.1175/1520-0493(2000)129<4097:TABIOA>2.0.CO;2.

Neumann, C. J., B. R. Jarvinen, C. J. McAdie, and G. R. Hammer, 1999: *Tropical Cyclones of the North Atlantic Ocean, 1871–1998*. National Oceanic and Atmospheric Administration, 206 pp.

Puri, K., J. Barkmeijer, and T. N. Palmer, 2001: Ensemble prediction of tropical cyclones using targeted diabatic singular vectors. *Quart. J. Roy. Meteor. Soc.*, **127**, 709-734.

Simmons A., S. Uppala, D. Dee, and S. Kobayashi, 2007: The ERA interim reanalysis. *ECMWF Newsletter*, No. 110, ECMWF, Reading, United Kingdom, 25–35.

Thorncroft, C., and K. Hodges, 2001: African easterly wave variability and its relationship to Atlantic tropical cyclone activity. *J. Climate*, **14**, 1166–1179.

Vitart, F., R. Buizza, M. Alonso Balmaseda, G. Balsamo, J.-R. Bidlot, A. Bonet, M. Fuentes, A. Hofstadler, F. Moleni, and T. Palmer, 2008: The new VAREPS-monthly forecasting system: A first step towards seamless prediction, *Quart. J. Roy. Meteor. Soc.*, **134**, 1789 – 1799, doi:10.1002/qj.322.

Vitart, F., 2009: Impact of the Madden-Julian Oscillation on tropical storms and risk of landfall in the ECMWF forecast system. *Geophys. Res. Lett.*, **36**, L15802, doi:10.1029/2009GL039089.

Wheeler, M. C., and H. H. Hendon, 2004: An all-season real-time multivariate MJO index: Development of an index for monitoring and prediction. *Mon. Wea. Rev.*, **132**, 1917–1932.

Wheeler, M., and G. N. Kiladis, 1999: Convectively coupled equatorial waves: Analysis of clouds and temperature in the wavenumber-frequency domain, *J. Atmos. Sci.*, **56**, 374–399.

Wilks, D. S., 1995: *Statistical Methods in the Atmospheric Sciences*. Academic Press, 467 pp.

Figure Captions

Fig. 1. (a) Variance from climatology (1970–2000) of TC probabilities in the ECMFS for the full 32-day period of monthly forecasts initialized on 7 August 2008 and one week later (b) on 14 August 2008. The observed tracks of tropical cyclones that occurred during each 32-day period are overlaid in black.

Fig. 2. Brier Skill Scores for the ECMFS as a function of weeks-in-advance. The weekly composites include all of the monthly forecasts made from June to October during 2008 and 2009. Weeks 1, 2, 3, and 4 cover days, 1-7, 8-14, 15-21, 22-28, respectively. Tropical cyclone climatology, which is determined using HURDAT for the period 1970-2000, is the reference forecast. Values above 0 indicate skill beyond climatology, and a value of 1 implies a perfect forecast. Note the Brier skill scores have been smoothed once by a 9-point running mean.

Fig. 3. Reliability diagram of the ECMFS as a function of weeks-in-advance. The inset has the relative occurrence frequency of each forecast TC probability level normalized by the size of the 0.25 x 0.25 grid domain. The reliability diagram is constructed using the full domain of the probability forecasts along with observations.

Fig. 4. Relative Operating Characteristic (ROC) of the ECMFS for the maximum TC forecast probabilities in the (a) Gulf of Mexico, (b) Caribbean Sea, (c) West Atlantic, and (d) Main Development Region as a function of weeks-in-advance. The diagonal, dashed line indicates no forecast skill.

Fig. 5. Correlation coefficients between the ECMFS and the ERA-Interim Reanalysis for deep-layer (850 –200 mb) vertical wind shear as a function of weeks-in-advance. The by-week composites include all of the weekly forecasts made from June to October of 2008 and 2009. Weeks 1, 2, 3, and 4 cover the days, 1-7, 8-14, 15-21, 22-28, respectively. Shaded regions are statistically significant at the 95% confidence level using a bootstrap resampling method.

Fig. 6. (a) Spatial correlation coefficients between forecast probability levels of tropical cyclone activity and the frequency of easterly waves in the ECMFS. Shaded regions are statistically significant at the 95% confidence level using a bootstrap resampling method. Time series of the correlation coefficients between the ECMFS and the ERA-Interim reanalysis for 850 hPa relative vorticity variance as a function of days in advance in the Main Development Region-MDR, East MDR, and West MDR (orange) for (b) 2008, (c) 2009, and (d) 2008–2009.

Fig. 7. Mean TC probability forecasts for the entire 32-day period from the ECMFS initialized when the convectively-active phase of the MJO with amplitude of at least one standard deviation was centered in (a) Regions 1 – 3 (Indian Ocean), (b) Regions 4 – 5 (Western Pacific), (c) Regions 6 – 8 (East Pacific/Western Hemisphere) at the time of model initialization. Mean TC probability forecasts as in panels a–c, except that the 32-day climatology of observed TC activity has been removed from each monthly forecast, for (d) Regions 1–3, (e) Regions 4–5, and (f) Regions 6–8. Note: The spatial probabilities have been smoothed once by a 9-point running mean.

Fig. 8. Conditional reliability of the TC probability forecasts from the ECMFS as a function of MJO location, at the time of model initialization. The inset is the relative occurrence frequency

of each forecast TC probability level normalized by the size of the 0.25 x 0.25 grid domain. The reliability diagram is constructed using the full domain of the probability forecasts along with observed TC activity for each 32-day period.

Fig. 9. Phase space diagrams of the Real-Time Multivariate MJO Series 1 & 2 for the period 1 June through 30 October for (a) 2008 and (b) 2009. MJO data obtained from Australia's Bureau of Meteorology. [Available online at http://www.cawcr.gov.au/bmrc/clfor/cfstaff/matw/maproom/RMM/]

Tables

Table 1: Relative operating characteristic (ROC) scores for TC probability forecasts within various regions of the North Atlantic including the Gulf of Mexico, Caribbean Sea, West Atlantic, and Main Development Region as a function of weeks-in-advance. Higher ROC scores indicate greater forecast skill, where 0.5 is the threshold for no forecast utility.

Relative Operating Characteristic (ROC)	Week 1	Week 2	Week 3	Week 4
Gulf of Mexico	0.85	0.66	0.60	0.64
Caribbean Sea	0.80	0.75	0.67	0.68
West Atlantic	0.87	0.81	0.65	0.72
Main Development Region	0.85	0.81	0.75	0.76

Figures

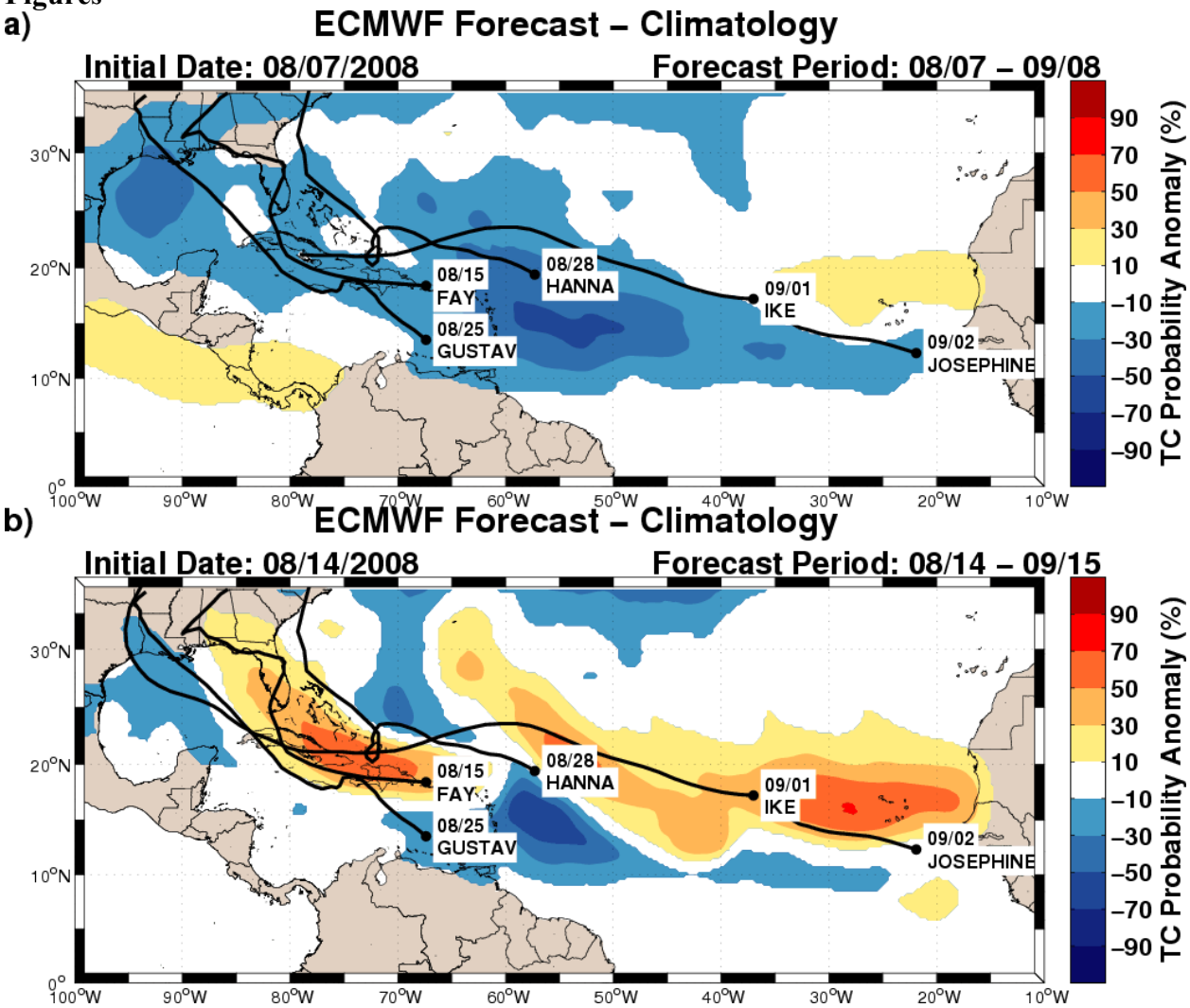

Fig. 1. (a) Variance from climatology (1970–2000) of TC probabilities in the ECMFS for the full 32-day period of monthly forecasts initialized on 7 August 2008 and one week later (b) on 14 August 2008. The observed tracks of tropical cyclones that occurred during each 32-day period are overlaid in black.

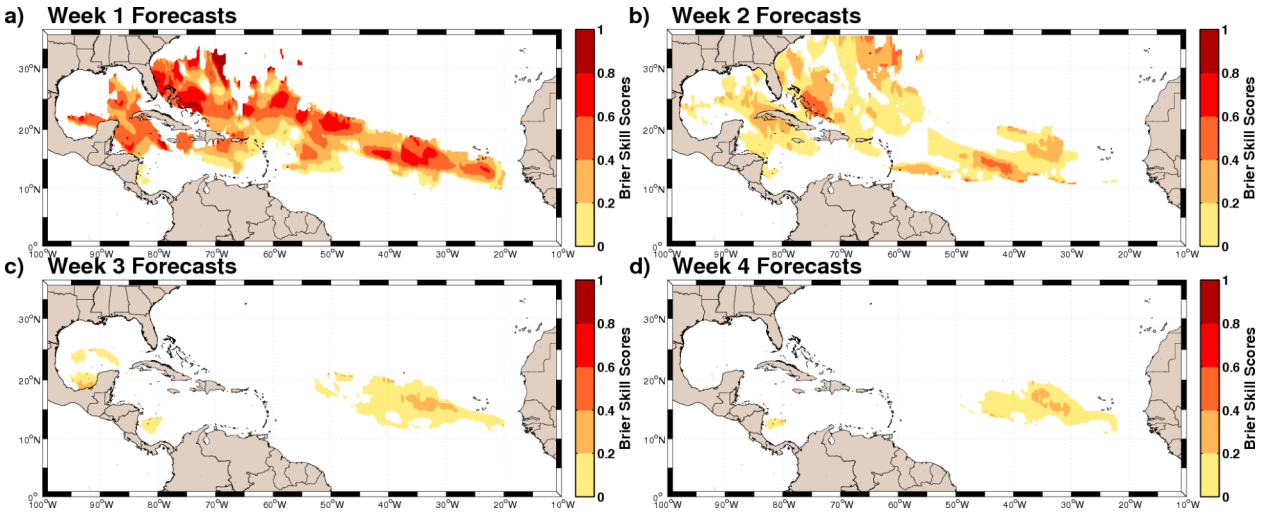

Fig. 2. Brier Skill Scores for the ECMFS as a function of weeks-in-advance. The weekly composites include all of the monthly forecasts made from June to October during 2008 and 2009. Weeks 1, 2, 3, and 4 cover days, 1-7, 8-14, 15-21, 22-28, respectively. Tropical cyclone climatology, which is determined using HURDAT for the period 1970-2000, is the reference forecast. Values above 0 indicate skill beyond climatology, and a value of 1 implies a perfect forecast. Note the Brier skill scores have been smoothed once by a 9-point running mean.

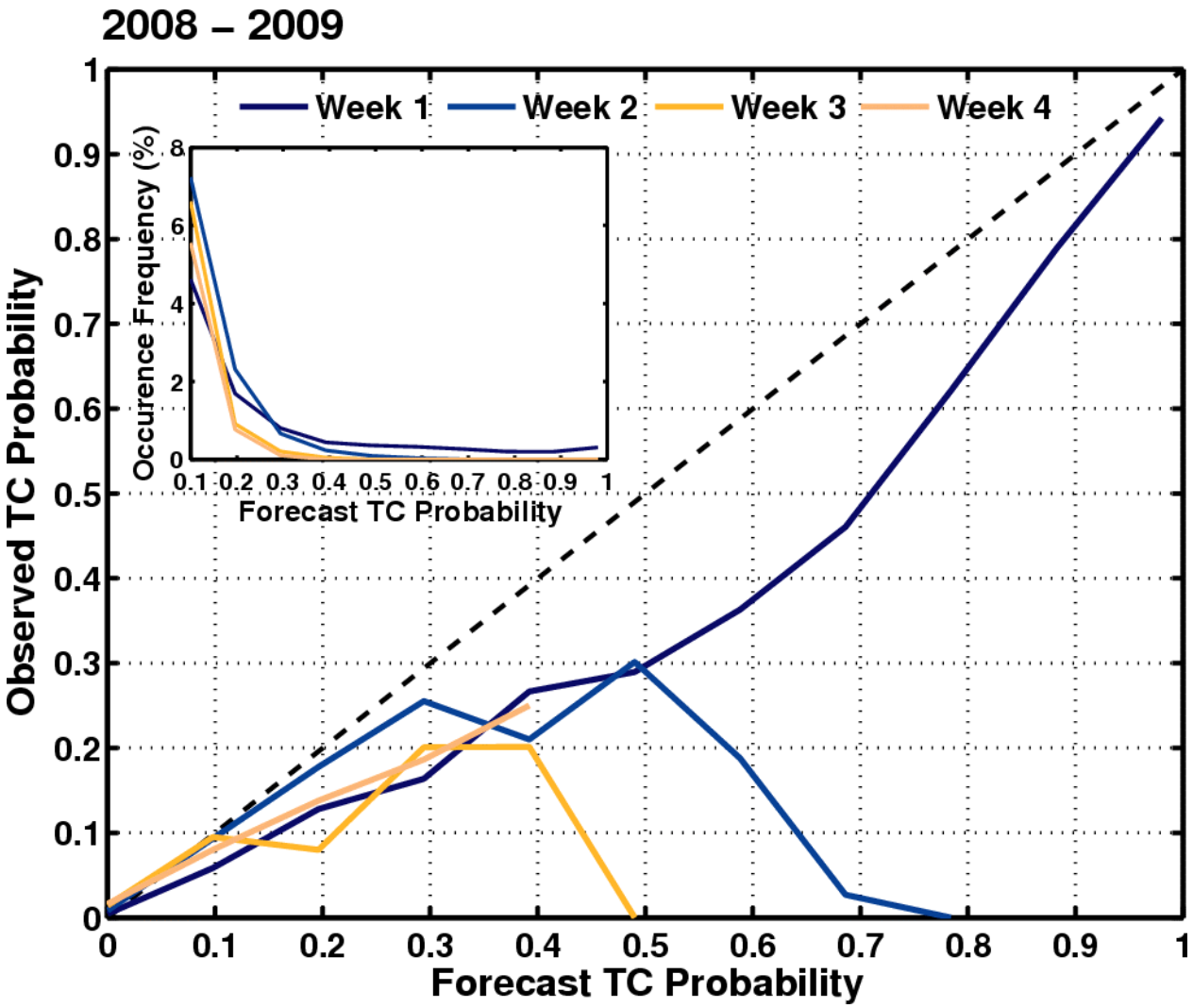

Fig. 3. Reliability diagram of the ECMFS as a function of weeks-in-advance. The inset has the relative occurrence frequency of each forecast TC probability level normalized by the size of the 0.25 x 0.25 grid domain. The reliability diagram is constructed using the full domain of the probability forecasts along with observations.

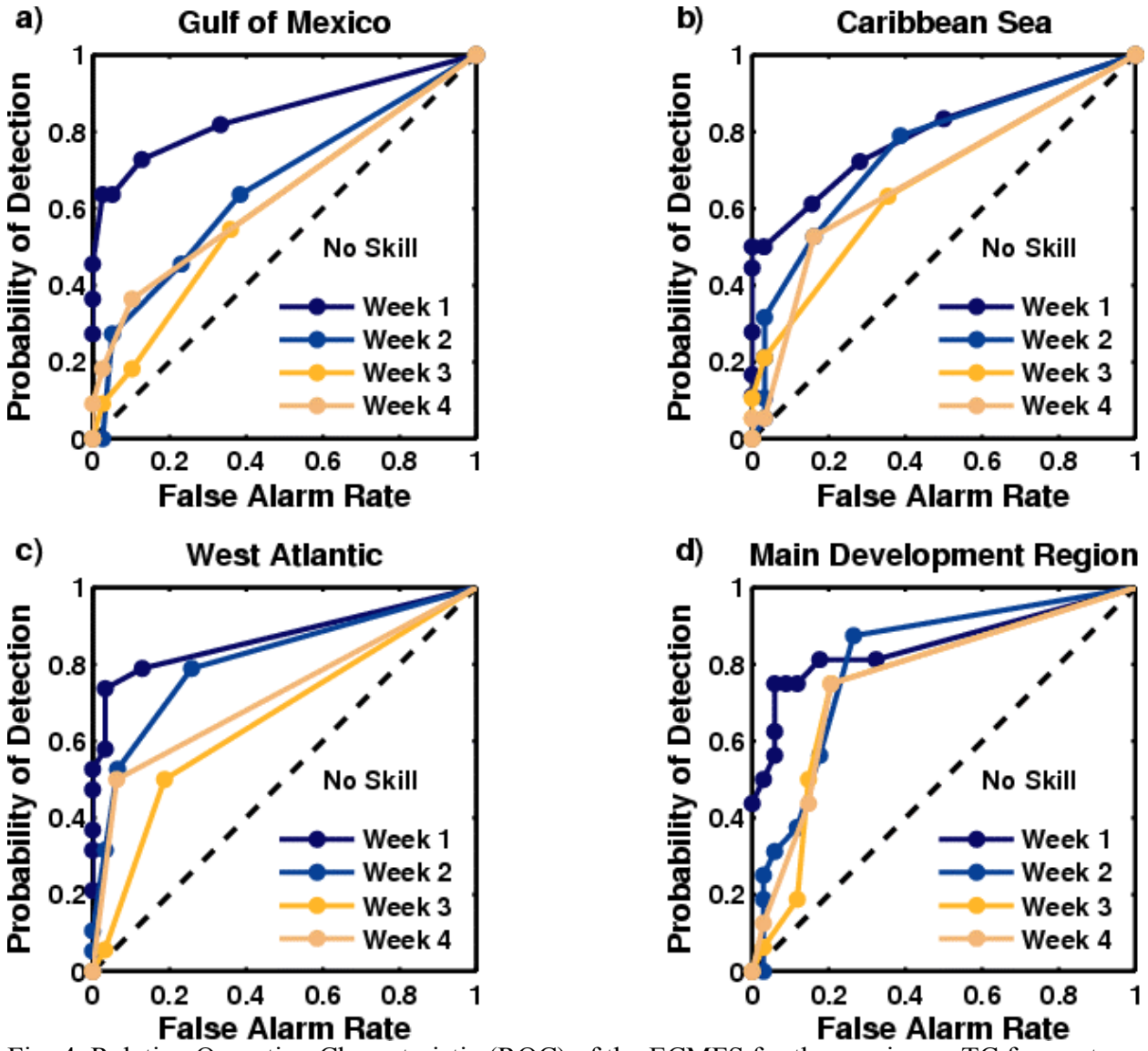

Fig. 4. Relative Operating Characteristic (ROC) of the ECMFS for the maximum TC forecast probabilities in the (a) Gulf of Mexico, (b) Caribbean Sea, (c) West Atlantic, and (d) Main Development Region as a function of weeks-in-advance. The diagonal, dashed line indicates no forecast skill.

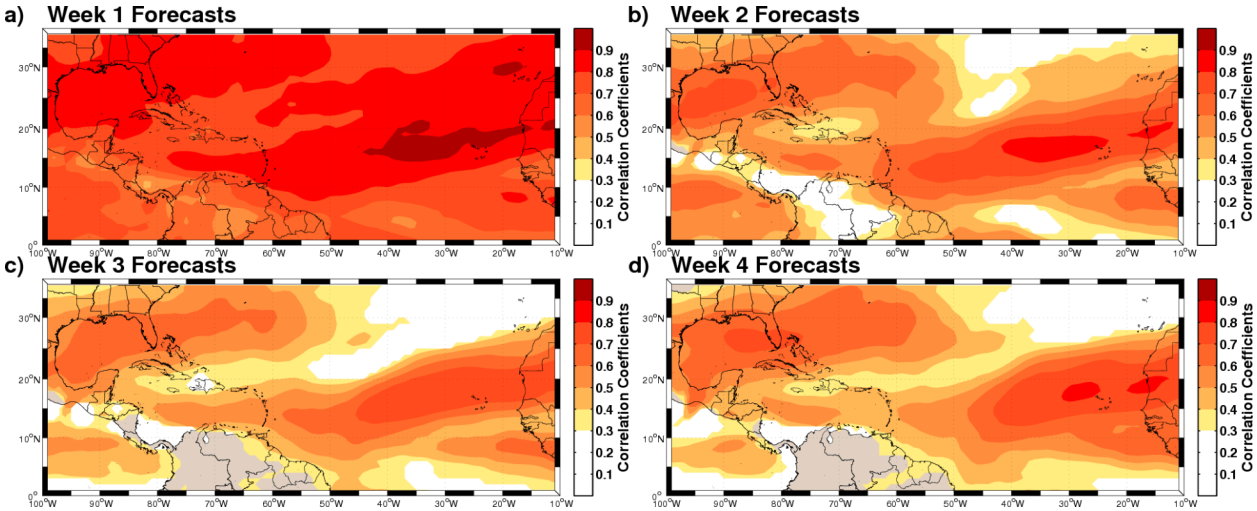

Fig. 5. Correlation coefficients between the ECMFS and the ERA-Interim Reanalysis for deep-layer (850 –200 mb) vertical wind shear as a function of weeks-in-advance. The by-week composites include all of the weekly forecasts made from June to October of 2008 and 2009. Weeks 1, 2, 3, and 4 cover the days, 1-7, 8-14, 15-21, 22-28, respectively. Shaded regions are statistically significant at the 95% confidence level using a bootstrap resampling method.

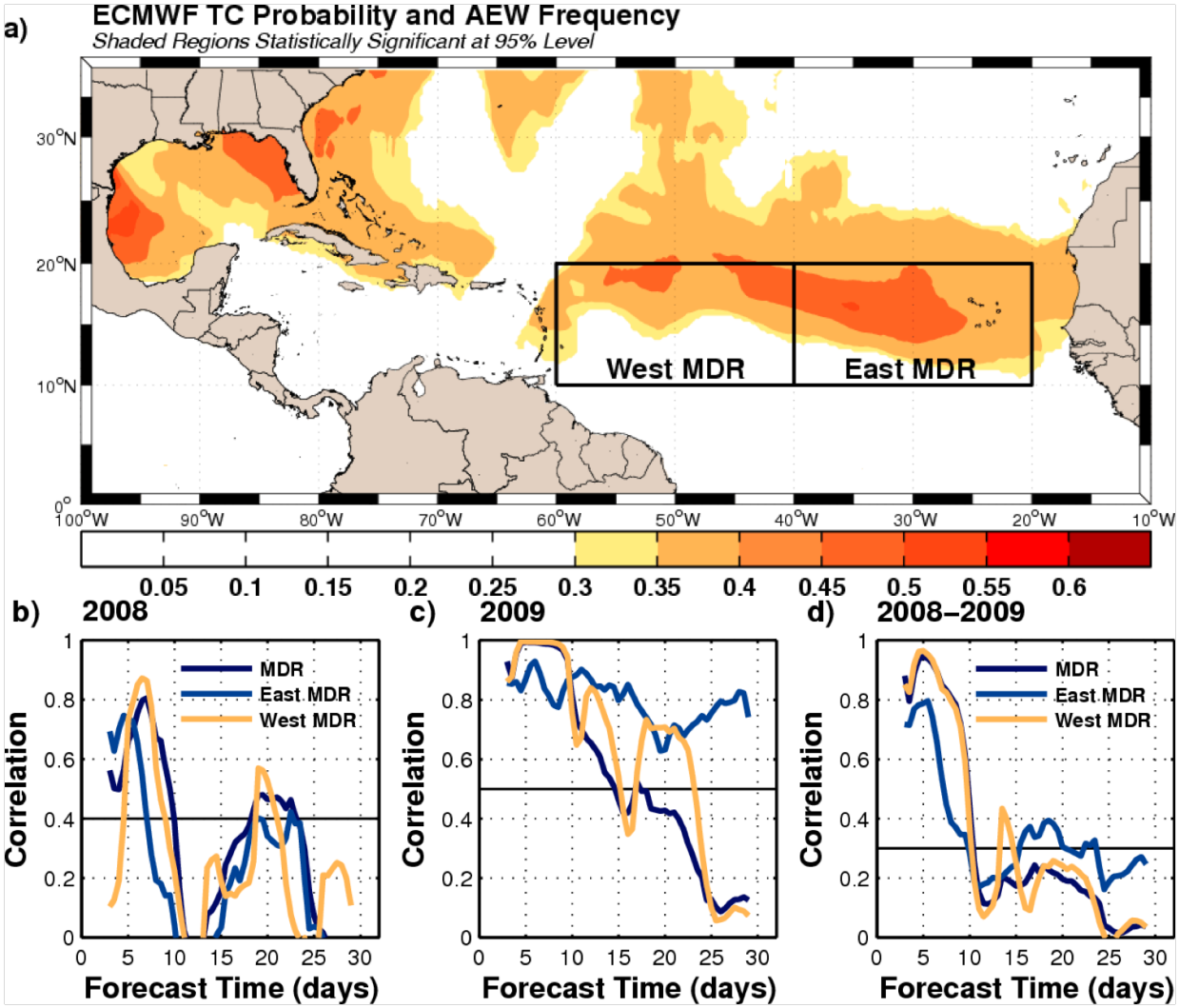

Fig. 6. (a) Spatial correlation coefficients between forecast probability levels of tropical cyclone activity and the frequency of easterly waves in the ECMFS. Shaded regions are statistically significant at the 95% confidence level using a bootstrap resampling method. Time series of the correlation coefficients between the ECMFS and the ERA-Interim reanalysis for 850 hPa relative vorticity variance as a function of days in advance in the Main Development Region-MDR, East MDR, and West MDR (orange) for (b) 2008, (c) 2009, and (d) 2008–2009.

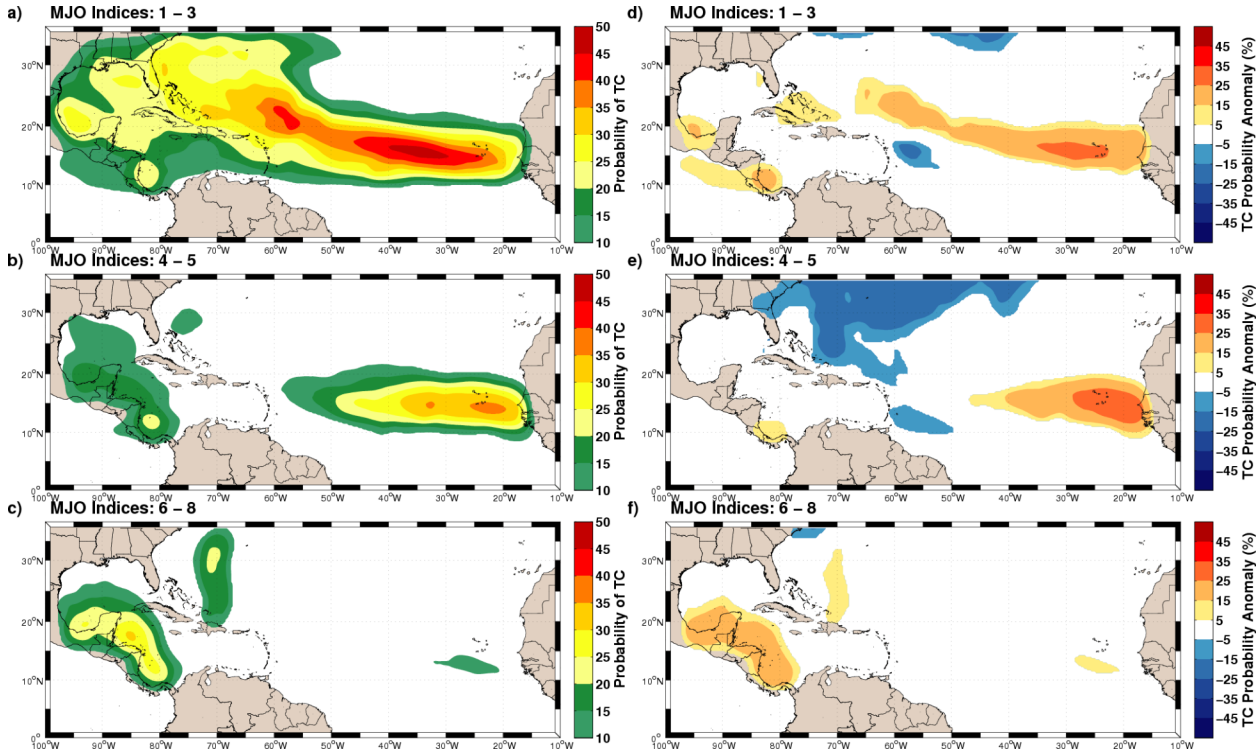

Fig. 7. Mean TC probability forecasts for the entire 32-day period from the ECMFS initialized when the convectively-active phase of the MJO with amplitude of at least one standard deviation was centered in (a) Regions 1 – 3 (Indian Ocean), (b) Regions 4 – 5 (Western Pacific), (c) Regions 6 – 8 (East Pacific/Western Hemisphere) at the time of model initialization. Mean TC probability forecasts as in panels a–c, except that the 32-day climatology of observed TC activity has been removed from each monthly forecast, for (d) Regions 1–3, (e) Regions 4–5, and (f) Regions 6–8. Note: The spatial probabilities have been smoothed once by a 9-point running mean.

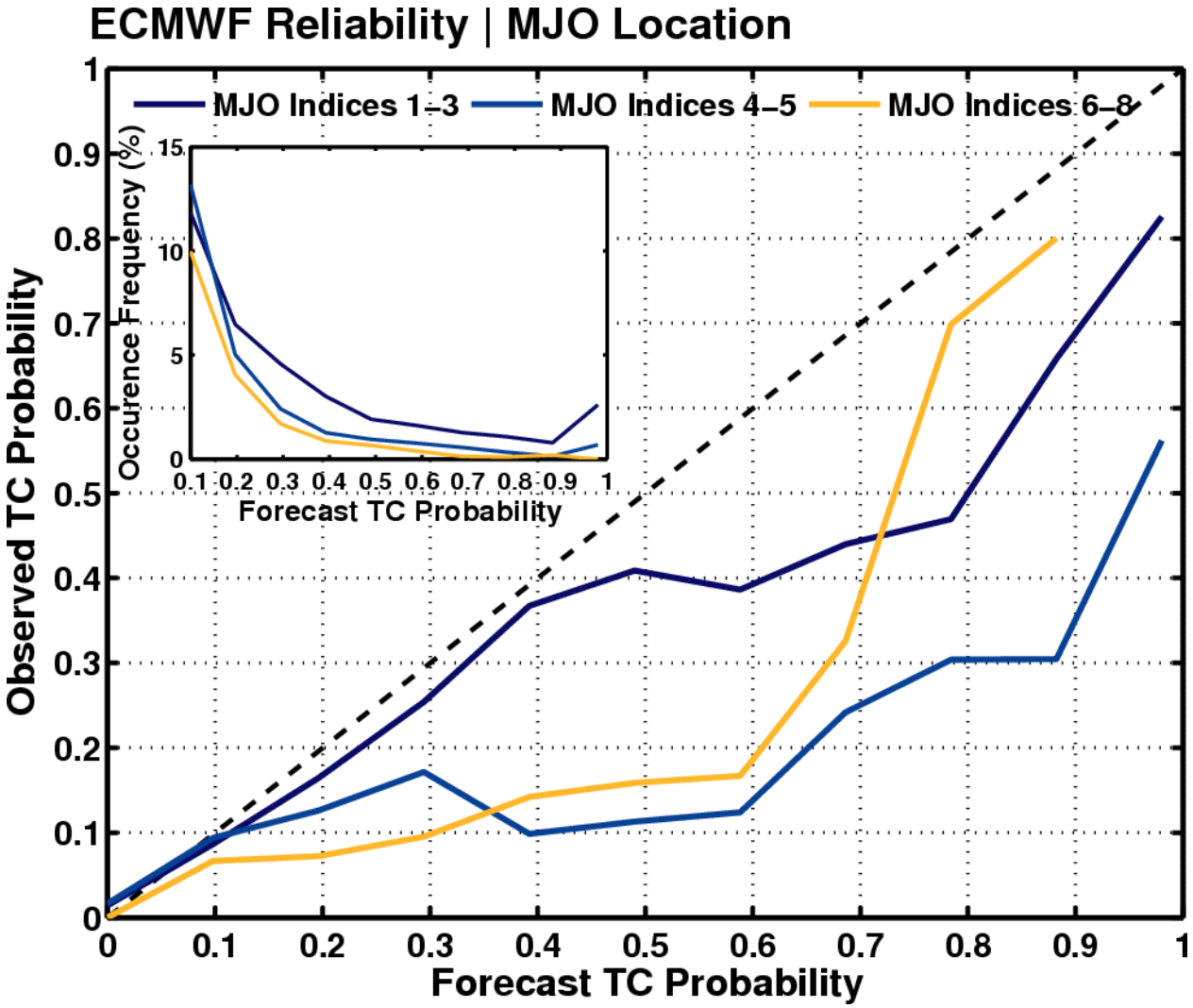

Fig. 8. Conditional reliability of the TC probability forecasts from the ECMFS as a function of MJO location, at the time of model initialization. The inset is the relative occurrence frequency of each forecast TC probability level normalized by the size of the 0.25 x 0.25 grid domain. The reliability diagram is constructed using the full domain of the probability forecasts along with observed TC activity for each 32-day period.

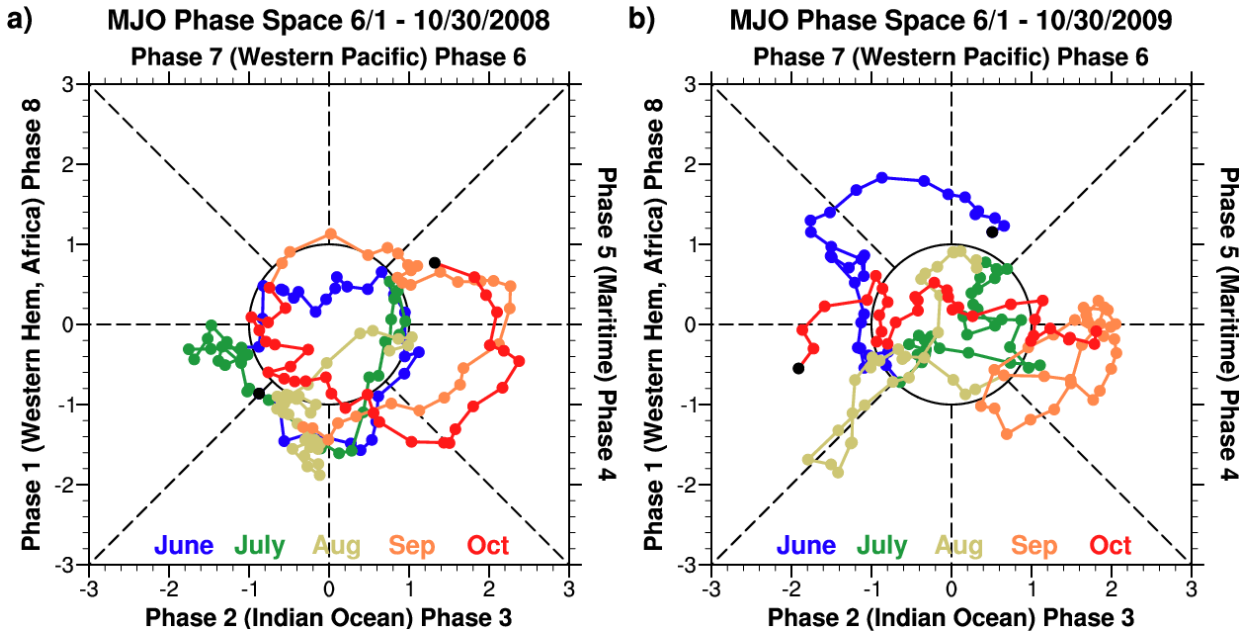

Fig. 9. Phase space diagrams of the Real-Time Multivariate MJO Series 1 & 2 for the period 1 June through 30 October for (a) 2008 and (b) 2009. MJO data obtained from Australia's Bureau of Meteorology. [Available online at http://www.cawcr.gov.au/bmrc/clfor/cfstaff/matw/maproom/RMM/]